PHIMO_FeCAP Compact Model
User Manual

Version: 1.0.0

Ning Feng, Ning Ji, Hao Li, Lining Zhang

September 2022

License

The terms under which the software and associated documentation (the Software) is provided are as the following:

DISCLAIMER: The Software is provided “as is” without warranty of any kind, express or implied, including but not limited to the warranties of merchantability, fitness for a particular purpose and noninfringement. In no event shall the authors or copyright holders be liable for any claim, damages or other liability, whether in an action of contract, tort or otherwise, arising from, out of or in connection with the Software or the use or other dealings in the Software.

Peking University grants, free of charge, to any users the right to modify, copy, and redistribute the Software, both within the user's organization and externally, subject to the following restrictions:

LIST OF CONDITIONS:

1. The users agree not to charge for the code itself but may charge for additions, extensions, or support.
2. In any product based on the software, the users agree to acknowledge the Research Group that developed the software. This acknowledgment shall appear in the product documentation.
3. Redistribution to others of source code must retain the copyright notice, disclaimer, and list of conditions.
4. Redistribution to others in binary form must reproduce the copyright notice, disclaimer, and list of conditions in the documentation and/or other materials provided with the distribution.

Contents

1 Introduction

A dynamic compact model, PHIMO_FeCAP is formulated for the FE capacitance in this document. It is derived from the state transition rate equations with clear physics beyond phenomenological models. Furthermore, minor loops are incorporated in the model based on domain interactions. The model is capable of covering the recently reported FE domain switching dynamics. Key features include:

1. The saturation and minor loops are calculated from the domain physics, including the domain parameter distributions and domain wall energy on the coercive voltage modulation.
2. A relaxation time approximation is used to develop the dynamic polarization formulation.
3. The dynamic model reproduces the experimental data well, and the model implementation facilitates circuit simulations.

2 FeCAP Compact Model

2.1 Parameters

Name	Description	Units	Reference	Default
L	length of fecap	m	2500×10^{-9}	/
W	Width of fecap	m	2500×10^{-9}	/
T_{fe}	Thickness of fe layer	m	4.0×10^{-9}	/
ε_o	Permittivity of vacuum	F/m	/	$8.854187817\times10^{-12}$
ε_{fe}	Permittivity of $Hf_{0.5}Zr_{0.5}O_2$	F/m	32	/
P_S	Saturated polarization	$\mu C/cm^2$	21	/
P_r	Remanent polarization	$\mu C/cm^2$	18	/
E_c	Coercive electrical	V/m	1.2×10^{8}	/
V_0	Related to the domain distributions	V	0.8	/
V_a	Related to intrinsic material properties	V	4.2	/
τ_0	Minimum time dependent on specific experimental devices	s	$6.43248008\ 13\times10^{-10}$	/
α	Fitting parameter	/	4	/

2.2 Model equations

2.2.1 Model Framework of State Transitions

A flow chart for the complete dynamic model is shown in Fig.1. The QS core calculates a voltage-forced polarization, and the NQS extension traces the actual dynamic polarization by a sub-circuit or a direct evaluation. The model implementation in Verilog-A is completed.

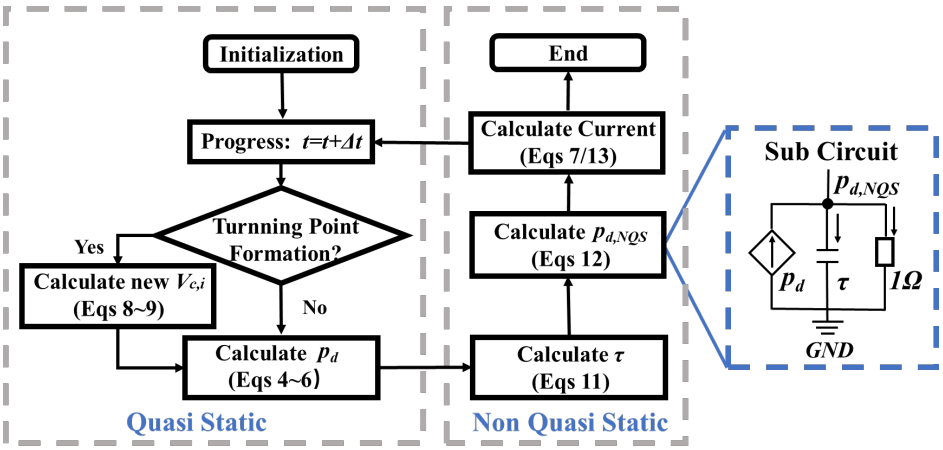

Fig. 1. A flow chart of the dynamic model calculations, including a quasi-static core module and a non-quasi-static module.

2.2.2 A Quasi-Static Core Module

Fig. 2 presents the state transition voltage domains. It is the multidomain property that leads to the fractional polarization state. The total ferroelectric polarization P is the superimposition of charges contributed by the two states and P_S represents the saturated polarization, $P = 2 \times p_d \times P_S - P_S$.

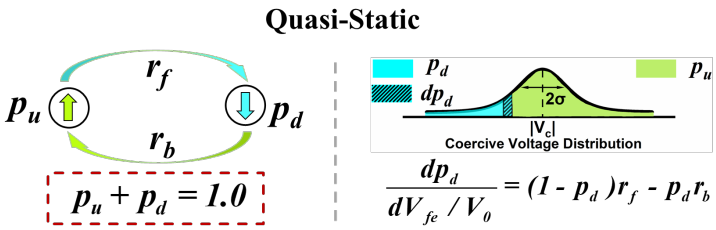

Fig. 2. Upward and downward polarizations, with their fractions pu and pd, respectively. The state transition in the time domain is defined by two transition rates depending on the applied voltage.

In the voltage domain, an analogy forward transition to the p_d state from the p_u state is given by r_f. It describes the incremental polarization due to the applied external voltage exceeding the coercive voltages of corresponding domains. The principle is explained in Fig.2, assuming a Gaussian distribution of coercive voltages as in literature [1], with V_c a mean coercive voltage, and σ the standard deviation. However, there are two issues in using the exact Gaussian distribution. One issue is that a negative coercive voltage is possible for the transition from upward to downward states. In this case, the central part of the distribution is focused. Another issue is that the obtained transition rate involves an error

function which hinders further model derivations. Consequently, an approximated distribution is then used leading to a simplified and approximation of r_f:

$$\mathrm{r}_f = \frac{1}{1+\exp[-(V_{fe}-V_c)/V_0]} \tag{1}$$

with V_0 related to the domain distributions $V_0=\sqrt{2\pi}\sigma/4$. Similarly, a backward transition r_b describes the cases when the applied voltage decreases.

A quasi-static (QS) core module under electric equilibrium is derived by considering the state transition with the voltage forces. The forward transition with increasing voltage is given by the differential equation:

$$\frac{dp_d}{dV_{fe}/V_0} = p_u r_f \tag{2}$$

and the backward transition is given by:

$$\frac{dp_d}{dV_{fe}/V_0} = -p_d r_b \tag{3}$$

With Eq. (1), Eq. (2) is integrated analytically with an assumed initial state (an applied voltage $V_{fe,i}$, and a downward polarization $p_{d,i}$). The solution is given by:

$$p_u = p_{u,i}\frac{1+\exp[(V_{fe,i}-V_c)/V_0]}{1+\exp[(V_{fe}-V_c)/V_0]} \tag{4}$$

Similarly, solving Eq. (3) leads to an analytical equation:

$$p_d = p_{d,i}\frac{1+\exp[-(V_{fe,i}+V_c)/V_0]}{1+\exp[-(V_{fe}+V_c)/V_0]} \tag{5}$$

The initial state ($V_{fe,i}$, P_i) within the saturation loop can be any state, e.g., (0.0, 0.0). It simplifies circuit simulations where voltage division occurs. A state with a possible depolarization field is stored after operations for analog memory. It is used as the initial state in the next operation. The initial state is also used to define the turning points. For the saturation loop, Eq. (5) is used after V_{fe} retreats from its peak value, with an initial state of $p_{d,i}$ = 1.0.

The total charge in the FE capacitance is obtained with contributions from a linear capacitance C_{fe}:

$$P_{fe} = (2p_d - 1) \cdot P_S + C_{fe} \cdot V_{fe} \tag{6}$$

where C_{fe} follows its traditional definition. The displacement current in the quasi-static case is calculated by:

$$i = \frac{dP_{fe}}{dV_{fe}} \frac{dV_{fe}}{dt} \tag{7}$$

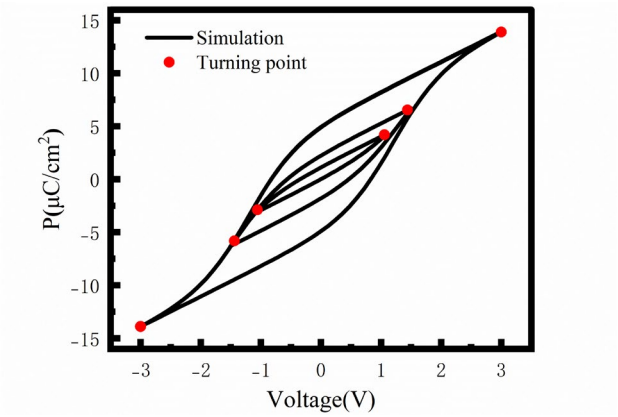

Fig. 3. Turning points diagram of Saturation loop and minor loop

The formation and wiping-out of turning points of the P-V hysteresis loops are defined with the classical protocol [2]. Assuming the new turning point is ($V_{fe,i}$, $p_{d,i}$) and the previous turning point is ($V_{fe,t}$, $p_{d,t}$), both are the solution of Eq. (4), with a new coercive voltage ($V_{c,i}$):

$$\frac{1 - p_{d,t}}{1 - p_{d,i}} = \frac{1 + \exp[(V_{fe,i} - V_{c,i}) / V_0]}{1 + \exp[(V_{fe,t} - V_{c,i}) / V_0]} \tag{8}$$

The solution of $V_{c,i}$ is analytically obtained:

$$V_{c,i} = V_0 \cdot \log[\frac{p_{u,t} \exp(V_{fe,t} / V_0) - p_{u,i} \exp(V_{fe,i} / V_0)}{p_{d,t} - p_{d,i}}] \tag{9}$$

2.2.3 A Non-quasi-static Module

At present, a simple rate is used with the reverse of switching time t_{sw} which represents the average relaxation time of the domain reversal [3]. When the external voltage is positive, the transition from the upward to downward state is dominant. However, the reversal transition is still possible due to thermal disturbance. Its transition rate r_{ud} is subject to a detailed balance principle (DBP), i.e., the polarization fraction under equilibrium is equal to that of the quasi-static case. When the external voltage is negative, the transition rates are defined

similarly.

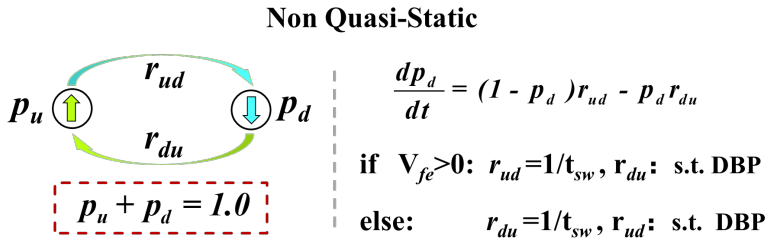

Fig. 4. The state transition in the time domain is defined by two transition rates depending on the applied voltage.

The non-quasi-static (NQS) module is derived with the state transition in the time domain. An ordinary differential equation is derived from the equations in Fig.4:

$$\frac{dp_{d,\mathrm{NQS}}}{dt} + \frac{p_{d,NQS}}{\tau} = \frac{1}{\tau}\frac{r_{du}}{r_{du} + r_{ud}} \tag{10}$$

in which a characteristic time τ is defined. For the case of nucleation limited switching (NLS), the characteristic time [3] as a function of voltage is given by:

$$\tau = \frac{1}{r_{ud} + r_{du}} \cong t_{SW} = \tau_0 \exp\left(\frac{V_a}{|V_{fe}|}\right)^{\alpha} \tag{11}$$

where V_a is related to intrinsic material properties including domain wall energy and portion of switched polarization by the nucleation. At the slow limit, $p_{d,NQS}$ reaches its quasi-static value p_d. Eq. (9) is rewritten as:

$$\frac{dp_{d,NQS}}{dt} + \frac{p_{d,NQS}}{\tau} = \frac{p_d}{\tau} \tag{12}$$

It is similar to a relaxation approximation in device modeling [4,5]. The domain switching takes a certain period and thus is not responding simultaneously to a fast-changing voltage. A deficit in polarization, $p_{d,def} = p_d - p_{d,NQS}$, is the driving force to complete the dynamic switching. The current is given by:

$$i = \frac{p_d - p_{d,NQS}}{\tau} \cdot 2P_s + C_{fe}\frac{dV_{fe}}{dt} \tag{13}$$

3 Examples

3.1 QS Module Simulation Example

The quasi-static module is verified to reproduce the measurement data of ferroelectric capacitance.

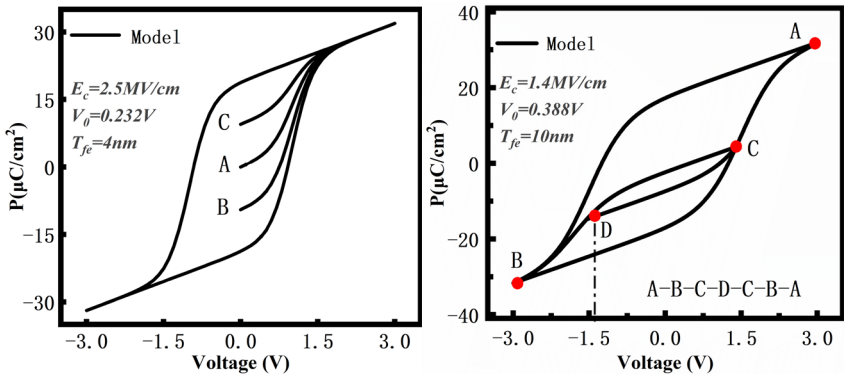

Fig. 5.(a) The model supports an initial state within the saturation loop, and (b) the model reproduces the minor loop trajectories [6] with modulations of coercive voltages.

Fig. 5(a) displays the polarization-voltage (P-V) curves from the above quasi-static model with three initial states assumed. Fig. 5(b) presents a minor loop property obtained from the model. With the formation of turning point C, Eq. (9) is used to derive the coercive voltage used in conjunction with Eq. (5) for the trajectory of (C-B). Similarly, the trajectory of (D-C) is defined in the same way with a new coercive voltage. This is in contrast to the phenomenological model [2], which calculates the minor loop simply based on scaling and shifting the points of saturation loop.

3.2 NQS Module Simulation Example

Figure 6. shows the P-V curve given under triangular voltage waveforms of three frequencies, as frequency increases from 1k to 500k Hz, the coercive voltage increases significantly.

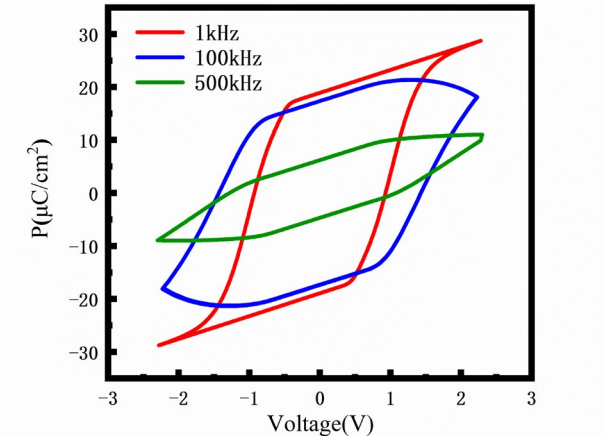

Fig. 6. P-V characteristics [8] under a high frequency (blue and green) show increased coercive voltages and reduced remnant polarization.

The pulse programming property of FE capacitance is further calculated in Fig. 7. It shows the switched fraction within a different width pulse.

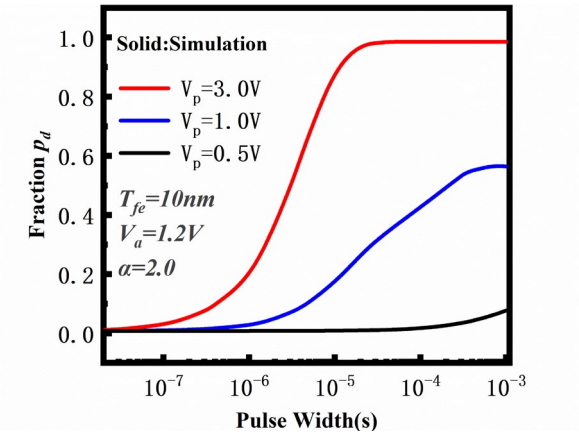

Fig. 7. Trade-off between pulse amplitude and width in programing from the model

After successfully establishing the FeCAP model, we can combine it with other components to build a hybrid structure like FeFET, FTJ, etc. Taking the FeFET as an example, a Fecap is connected in series with a transistor represented by the BSIM model. The transfer characteristics were measured from applying a voltage to the FeFET in the off state. Figure 8 shows the gate voltage and polarization in FeCAP as a function of time.

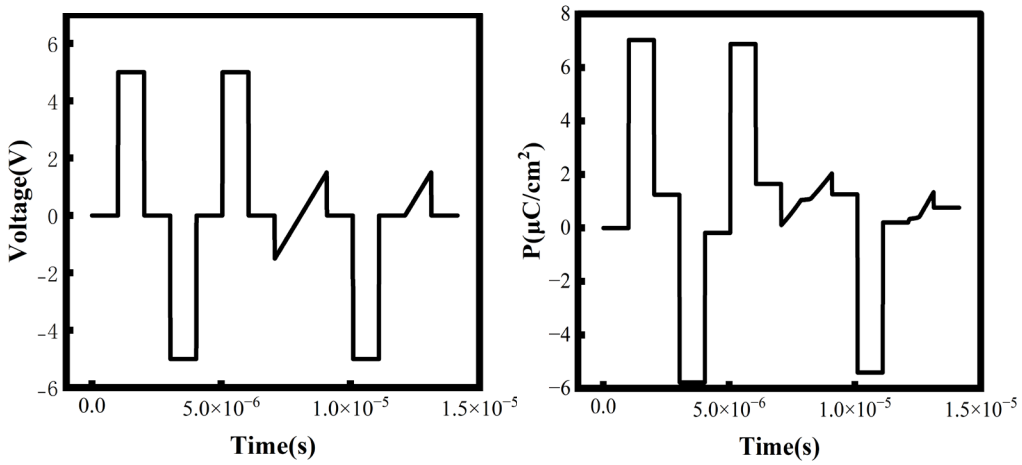

Fig. 8. (a) Gate pulse voltage diagram (b) Variation of FeCAP polarization with time.

As shown in Fig. 9, applying a negative pulse voltage (program operation) on the gate of the HZO-based FeFET induces the ferroelectric polarization to upward ($P\uparrow$), leading to a high V_{TH} state (red curve) or a small drain current (I_D). While the polarization aligns downward ($P\downarrow$) after applying a positive gate pulse voltage (erase operation), obtaining a low V_{TH} state (blue curve) or a large I_D.

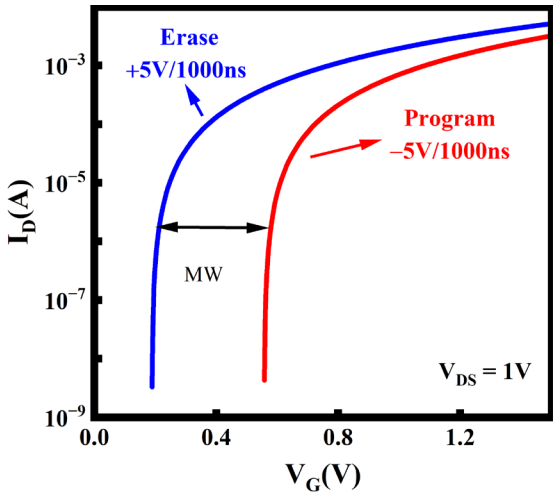

Fig. 9. I_D - V_G curves of the FeFET after applying a +5 V/1000 ns erase and a −5 V/1000 ns program pulse.

4 References

[1] C.Alessandri, P.Pandey, A.Abusleme, A.Seabaugh, “Monte Carlo simulation of switching dynamics in polycrystalline ferroelectric capacitors,” *IEEE Trans. Electron Devices*, vol. 66, no. 8, pp. 3527-3534, August 2019, doi: 10.1109/TED.2019.2922268.

[2] B, Jiang, P. Zurcher, R. Jones, S. Gillespie and J. Lee, "Computationally efficient ferroelectric capacitor model for circuit simulation,” *1997 Symposium on VLSI Technology,* 1997, pp. 141-142, doi: 10.1109/VLSIT.1997.623738.

[3] H.Mulaosmanovic, J. Ocker, S. Müller, U. Schroeder, J. Müller, P. Polakowski, S. Flachowsky, R. Bentum, T. Mikolajick, and S. Slesazeck, “Switching kinetics in nanoscale hafnium oxide based ferroelectric field-effect transistors,” *Applied Materials Interfaces*, vol. 9, no. 4,pp.3792–3798, Feb,2017. doi: 10.1021/acsami.6b13866.

[4] M. Chan, K. Y. Hui, C. Hu, and P. K. Ko, “A robust and physical BSIM3 non-quasi-static transient and AC small-signal model for circuit simulation,” *IEEE Trans. Electron Devices*, vol. 45, no. 4, pp. 834–841,Apr. 1998. doi: 10.1109/16.662788.

[5] H. Hu, D. Liu, X. Chen, D. Dong, X. Cui, M. Liu, X. Lin, L. Zhang, M. Chan, “A Compact phase change memory model with dynamic state variables,” *IEEE Trans. Electron Devices*, vol. 67, no. 1, pp. 133–139, Jan. 2020. doi: 10.1109/TED.2019.2956193.

[6] K. Ni, M. Jerry, J. A. Smith and S. Datta, "A circuit compatible accurate compact model for ferroelectric-FETs,” *2018 IEEE Symposium on VLSI Technology*, 2018, pp. 131-132, doi:10.1109/VLSIT.2018.8510622.